他誌発表論文 再録
公益社団法人計測自動制御学会
Journal of Control, Measurement, and System Integration (JCMSI) Vol.17 No.1 p 256-, 263 2024

SICE JOURNAL OF CONTROL, MEASUREMENT, AND SYSTEM INTEGRATION
2024, VOL. 17, NO. 1, 256–263
https://doi.org/10.1080/18824889.2024.2366554

Usefulness of hand sensor device for lumbar load estimation

Yusuke Yoshida[a], Takashi Kamezaki[a], Dai Kinoshita[b] and Daisuke Kushida[c]

[a]Machinery & Materials Research Laboratory, Tottori Institute of Industrial Technology, Tottori, Japan; [b]National Institute of Technology, Yonago College, Tottori, Japan; [c]Faculty of Engineering, Tottori University, Tottori, Japan

ABSTRACT

We have developed a novel hand sensor device designed to mitigate sensor malfunction caused by palm bending and to adjust output values by considering palm hardness. The primary goal of this device is not to acquire accurate hand load values but rather to gather pertinent information for estimating the lumbar load. Therefore, leveraging the load and posture data captured by this sensor, we endeavoured to estimate the electromyography (EMG) value – specifically the muscle action potentials in the lumbar region – using myoelectric potential sensors and adopting deep learning methodologies. The estimated values closely matched the EMG results and demonstrated a strong correlation with actual measurements of vertical luggage movement. Additionally, the usefulness of the hand sensor device was validated through simulations conducted with varying levels of information, thereby elucidating the impact of explanatory variables used in the estimation process.

ARTICLE HISTORY
Received 30 October 2023
Revised 9 April 2024
Accepted 5 June 2024

KEYWORDS
Hand sensor; inertia sensor; myoelectric potential sensor; lumbar load; recurrent neural network; lumbar load estimation

1. Introduction

Regarding the number of occupational illnesses resulting in four or more days of absence from work, as compiled by the Ministry of Health, Labor, and Welfare, back pain accounts for approximately 60% of cases annually [1]. Nursing care is the most common occupation, with more than 70% of nursing care workers experiencing back pain [2]. As the population ages, labour shortages become more pronounced, posing challenges in securing adequate human resources, particularly if back pain issues persist unresolved. Therefore, it becomes crucial to predict and comprehend the tasks that contribute to back pain, emphasizing the necessity of measuring lumbar load, especially during activities involving heavy lifting.

Over the years, extensive research has been conducted to the body's condition, leading to reports on work posture estimation [3] and the relationship between work postures and low back pain [4]. Muscle activity is typically measured using myoelectric potential sensors to determine bodily dynamics [5]. These sensors capture changes in the skin's electrical potential caused by muscle activity (EMG: Electromyography). EMG is widely recognized as a reliable indicator of muscle activity [6]. However, the challenge arises from the necessity of directly attaching the myoelectric potential sensor to the skin with adhesive tape, which can weaken due to repeated movements or perspiration, leading to increased contact resistance and compromising the accuracy of measurements. Therefore, ensuring accurate measurements over an extended period becomes crucial.

However, since the load exerted on the body is predominantly transmitted through the sole, there has been a development of sensors capable of measuring sole load, leading to numerous studies [7] and commercial applications. However, when carrying heavy objects, the lumbar load varies with different postures. Therefore, while knowledge of sole load is valuable, it alone is insufficient to accurately estimate the lumbar load on the lower back. Therefore, it becomes essential to measure the load applied to the hands, corresponding to the force point. Various devices, such as grasping pressure distribution sensors [8] and high-density conformable tactile sensing gloves [9], have been explored for hand load measurement. However, these devices, tailored for precise grasping load measurement, present issues such as sensor disconnection due to grasping, lack of strength against heavy objects, and difficulty in detaching owing to their intricate arrangements. Therefore, they lack practicality for repeated use by workers for general purposes.

Therefore, our endeavour focused on estimating lumbar load during heavy object grasping by employing deep learning techniques. This involved utilizing load information applied to both hands, measured through a pressure-sensitive conductive elastomer, along with posture data obtained from an inertial sensor. The development conditions for the hand sensor device utilized in this study were as follows:

CONTACT Yusuke Yoshida yoshida-yu@tiit.or.jp

Figure 1. Pressure-sensitive conductive elastomer.

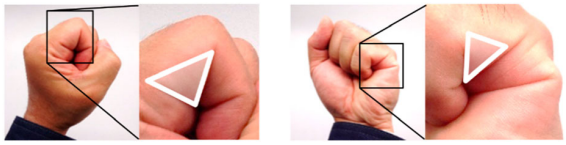

Figure 2. Sides of clenched fist.

(1) Measuring long working hours at all times
(2) Ease of detachment
(3) Not obtaining accurate hand load values, but rather to gather the essential information required for lumbar load estimation.

The accuracy of a hand sensor device, designed to gather information crucial for lumbar load estimation, was verified through simulations [10]. However, this study did not address the extent of influence exerted by the explanatory variables used in the estimation process, leaving the usefulness of the hand sensor device ambiguous. To address this gap, the current study discusses the efficacy of each sensor by estimating lumbar load with reduced information on explanatory variables, supplementing the previous validation efforts.

2. Development of hand sensor device

2.1. Consideration of sensor placement locations

A pressure-sensitive conductive elastomer (Figure 1), utilized as a pressure sensor in hand sensor devices, exhibits changes in resistance not only in response to compressive forces but also to bending, thereby altering its outputs value. Deciphering the specific data causing resistance changes posed a challenge. Therefore, it became imperative to minimize sensor output attributed to bending in pressure sensors intended for hand sensor devices. As illustrated in Figure 2, when the hand clenches, the joints and the skin surface between them contort into a triangular shape. Placing a pressure-sensitive conductive elastomer in this area results in output value fluctuations by finger movements, even in the absence of external loads. However, the areas exhibiting less deformation during hand movement are limited. The finger pulp (blue), fingertip (green), thenar (orange), and hypothenar (red) [11] are viable locations for sensor placement.

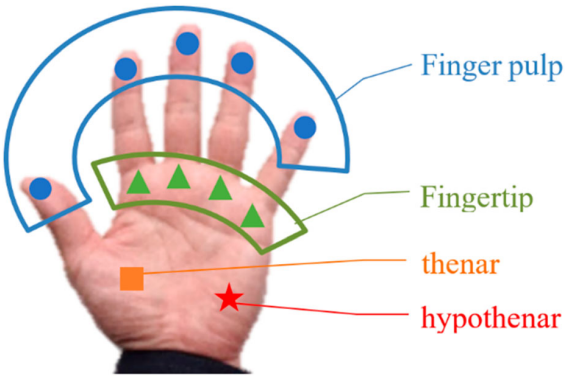

Figure 3. Areas with slight deformation of skin surface.

Table 1. Hardness of palm part.

Part	Asker type C*1 hardness (A_C)
Finger pulp	5
Fingertip	15
Thenar	5
Hypothenar	5

*1: Asker Type C is a type of Asker durometer specifically designed for measuring the hardness of soft rubber and sponges.

Subsequently, our attention turned to the properties of the pressure-sensitive conductive sensors. Generally, sensors undergo calibration using a hardboard. Therefore, when measuring pressure on a palm with a surface of different softness and hardness levels depending on its location, accurate pressure readings may not be measured [12]. As depicted in Table 1, the hardness of the proposed sensor arrangement candidates presented in Figure 3 is described in terms of Asker Type C hardness (A_C). Consequently, upon comparing the fingertips near the bone with areas like the finger pulp or thenar, which are less influenced by bone structure, differences in hardness became evident.

Therefore, the pressure-sensitive conductive sensor shown in Figure 3 was situated on gel-like materials characterised by A_C values of 4, 15, 20, and 30. The variation in resistance upon force application is illustrated in Figure 4, where the horizontal axis represents the applied force and the vertical axis denotes the sensor's resistance. The figure reveals minimal alteration at $A_C \geq 20$; however, distinct resistance variations were observed at AC < 20, even under identical force application. Additionally, the occurrence of hysteresis is evident due to the inherent nature of the sensor.

Figure 5 shows the relationship between hardness and sensor resistance at a load of 3 N, corresponding to the data illustrated in Figure 4. The horizontal and vertical axes represent hardness and resistance, respectively. The dashed line approximates a straight line as a function of A_C, indicating a proportional relationship between the sensor's resistance and hardness.

Let R_{min} represent the minimum resistance observed during calibration on a hard board, and let R denote

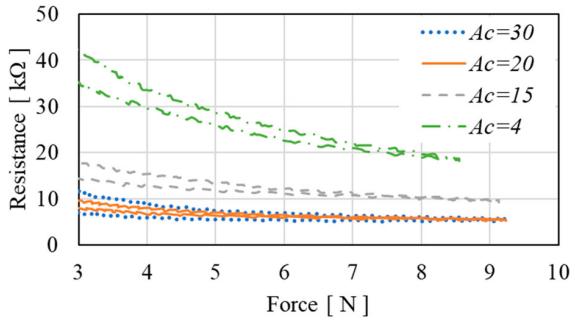

Figure 4. Force vs. sensor sensitivity.

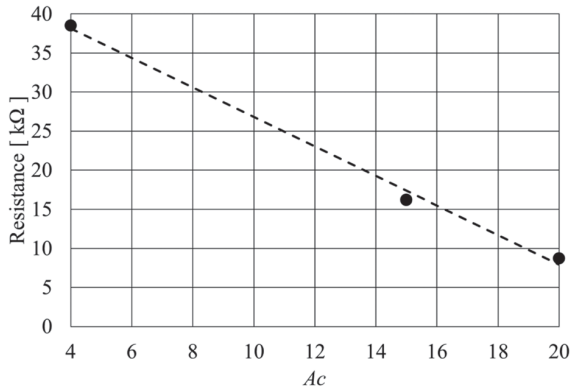

Figure 5. Hardness vs. resistance.

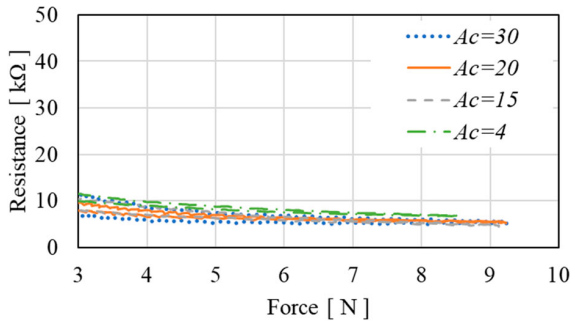

Figure 6. Correction results.

the resistance at hardness A_C ($A_C < 20$). The corrected resistance, RC, can be expressed using the following experimental formula:

$$R_C = (R - 2R_{min}) \times \left(\frac{Ac}{20}\right) + R_{min}.$$

A hardness-independent relationship between the load and sensor resistance can be achieved by adjusting this relationship, as illustrated in Figure 6. Furthermore, a reduction in hysteresis was observed. In this study, the attained accuracy was deemed sufficient, given that the primary goal was not to ascertain the precise load value exerted on the hand, but rather to accurately obtain the load information required for estimating lumbar loading.

Based on these results, we attached the existing pressure-sensitive conductive elastomer, as illustrated

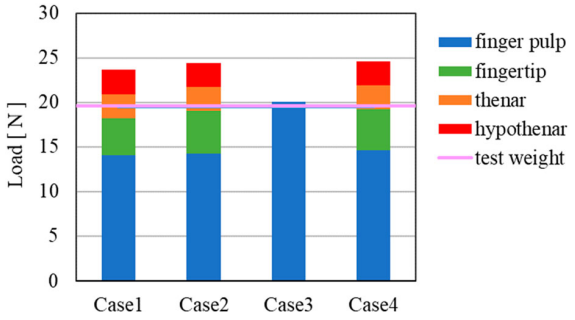

Figure 7. Examination results of sensor placement location.

Table 2. Experimental conditions.

Case1	Case2	Case3	Case4
			

in Figure 1, to the sensor placement positions outlined in Figure 3. Subsequently, we conducted an experiment involving gripping a 19.6 N box using the four configurations presented in Table 2. The load measurement results for each configuration are depicted in Figure 7. Interestingly, utilizing either fingertip or thenar + hypothenar locations yielded similar readings to the test weight. Given the expectation that the thenar and hypothenar muscles would remain unresponsive to posture changes, the finger pulp and fingertip emerged as the identified locations for load sensor attachment on the hand sensor device, based on the outcomes of the experiment.

2.2. Structure and features of load sensor

Existing pressure-sensitive conductive elastomers have circuit boards comprising flexible printed circuits (FPCs). When fabricated into a glove, it does not fit well because of its stiffness, and its shape must conform to that of a glove. Therefore, we developed a novel sensor. The sensor structure is a structure in which the pressure-sensitive conductive elastomer (Inastomer: manufactured by INABA RUBBER CO., LTD.) and the circuit part printed with silver nanopaste on a 0.1-mm-thick TPU sheet are cut into the shape of a glove overlap, as illustrated in Figure 8.

Furthermore, when the silver nanopaste circuit pattern was arranged in a comb shape, the wire broke only in the direction from the bend to the first joint and broke. As demonstrated in Figure 9, the wire broke only when the tip of the sensor was bent at the first joint. Therefore, the sensor did not lose its functionality.

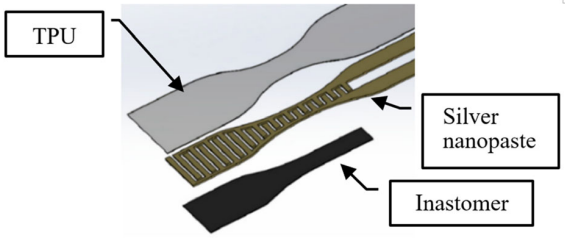

Figure 8. Sensor structure to acquire load information.

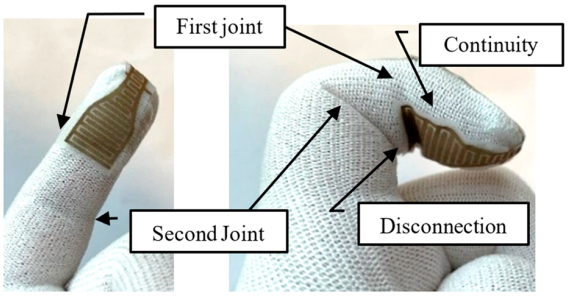

Figure 9. Example of disconnection.

2.3. Attitude information acquisition utilizing inertial sensors

To estimate lumbar load, posture information is required in addition to load information on the hands. This is because lumbar load differs depending on whether it is supported near the body or at a certain distance. Therefore, a nine-axis inertial measurement unit (IMU) comprising an acceleration sensor (three axes), gyro sensor (three axes), and magnetometer (three axes) was utilized to obtain posture information such as palm inclination and hand position. The posture information obtained from the nine-axis IMU comprises the quaternion q, which indicates the tilt of the palm calculated from the nine axes and the position information obtained by integrating the acceleration sensor values twice. The quaternion q is obtained from the scalar part q_0 and the vector parts q_1, q_2, and q_3 in

$$q = [q_0, q_1, q_2, q_3]^T.$$

2.4. Prototype of hand sensor device

We developed a prototype for a flexible and detachable hand sensor device, as illustrated in Figure 10. This device features six pressure-sensitive conductive sensors placed on the pulp and fingertips of each finger. Mounted on the back of the hand are a nine-axis IMU (BOSCH BNO055) and a microcomputer board (Espressif ESP32-DevKitC-32D), which can transmit the collected sensor data via Bluetooth low energy (BLE). Moreover, the same model of the nine-axis IMU was employed to monitor waist movement.

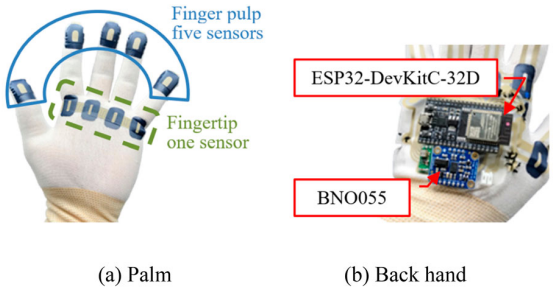

Figure 10. Prototype of hand sensor. (a) Palm; (b) Back hand.

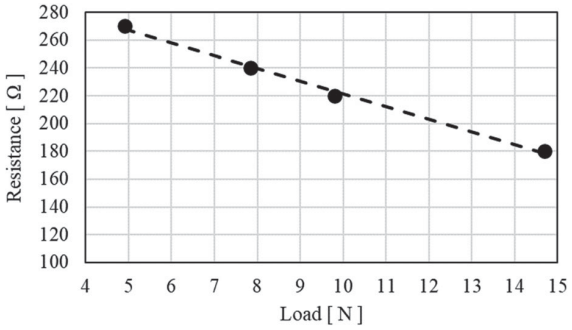

Figure 11. Load vs. resistance value.

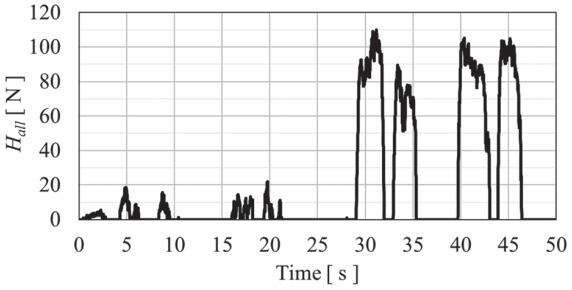

Figure 12. Measurement results of time series data.

2.5. Evaluation of prototype hand sensor device

Figure 11 illustrates the change in resistance observed in the prototype hand sensor device upon the application of a load to the index finger. The horizontal axis represents the applied load, while the vertical axis represents the resistance of the sensor device. Our findings confirm the linearity of the output values within the range of 4.9–14.7 N.

Next, 9.8 and 98 N loads placed on the floor were lifted with both hands, placed on the table, and then lowered again to the floor with the hand sensor device attached; each action was repeated twice. The total output value, H_{all}, was obtained from the output values of the left-hand H_L and right-hand H_R utilizing Eq. 1. Here, we set $K_1 = 0.7$ and $K_2 = -2.5$ and performed level matching with the actual load. The results are presented in Figure 12. The horizontal axis represents time, and the vertical axis represents the load value obtained

Table 3. Sensors utilized for estimation by deep learning.

	Data for lumbar load estimation		Data for learning
Type	Pressure sensor	Nine-axis IMU	EMG
Position			
Number	12 (6 × 2)	3 (2 + 1)	1
Data type	Load:*F*	Acceleration: a_{xh}, a_{yh}, a_{zh} Quaternion: q_1,q_2,q_3,q_4	EMG: *E*
Output	12	21	1

from Eq. 1.

$$H_{all} = K_1 \sum_{i=1}^{6} (H_{Li} + H_{Ri}) + K_2 \tag{1}$$

However, it was observed that $H_{all} \geq 0$. These results affirm the linearity of the prototype hand sensor device.

3. Lumbar load estimation utilizing hand sensor device

3.1. Experimental conditions

As illustrated in Table 3, 33 data points were used for estimating lumbar load. This comprised 12 data points for Load F acquired from the hand sensor device on both hands, and 21 data points encompassing three-axis acceleration (a_{xh}, a_{yh}, and a_{zh}) and quaternion (q_1, q_2, q_3, and q_4) gathered from the nine-axis IMU installed on both hands and waist. Additionally, EMG readings of the erector spinae muscle were taken, assuming a proportional relationship between lumbar load and muscle activity. Due to the absence of left/right movements during the simple up-and-down motion, EMG measurements were conducted on one side only. The recorded EMG values were processed to derive Root Mean Square (RMS) data with an averaging window of 500 ms. The data collection method for the lumbar load estimation experiment proceeded as follows:

(1) Grasp the luggage on the table.
(2) Place the luggage on the feet and let it go.
(3) Grasp the luggage on the feet.
(4) Place the luggage on a table and let it go.
(5) Repeat Steps 1–4 ten times.

Two distinct loads were used: a lighter load of 9.8 N and a heavier load of 98 N. Furthermore, two distinct postures were adopted for upward and downward movements of the load, as illustrated in Figure 13: bending and extending the knees, and stooping without bending the knees. Subjects were selected from the pool of authors, and careful ethical considerations were ensured throughout the study.

(1) Bending knees (2) Stooping (3) Lifting

Figure 13. Postures for moving load up and down. (1) Bending knees; (2) Stooping; (3) Lifting.

Table 4. Deep learning parameters.

Learning times	100epoch
Dropout rate	0.5
Number of training data points	33,097
Number of data points for verification	9838

The neural network model adopted for estimating lumbar load was a recurrent neural network (RNN)-based deep-learning approach, tailored for estimating relatively short time-series data. To enable calculations on the microcomputer, we optimized the model size by utilizing four hidden layers with 33 inputs and one output, as illustrated in Figure 14. Model construction involved simulating multiple variants using the neural network console developed by Sony Network Communications Inc., and the model exhibiting the highest validation accuracy was adopted. To prevent over-fitting, the learning rate was adjusted. Table 4 presents the deep learning parameters for the activation function *f*, as expressed by the following equation:

$$f(\alpha, n) = \begin{cases} \alpha n, & n < 0 \\ n, & n \geq 0 \end{cases}.$$

A parametric rectified linear unit (PReLU) was employed over a standard rectified linear unit (ReLU), commonly utilized in deep learning, because ReLU tends to nullify negative values of the input data. In each layer of the neural network structure, the alpha parameter of the PReLU was automatically adjusted during simulation using a neural network console. This approach enabled the determination of the optimal solution for each layer, enhancing the model's performance.

3.2. Estimation result utilizing deep learning

Eight out of the ten measurements were adopted as training data, while the remaining two were designated for validation purposes. The validation results are presented in Figure 15, where the horizontal axis represents time, and the vertical axis signifies the lumbar load. The EMG measurement results (blue) and the deep learning estimation results (orange) are plotted for comparison. Consequently, even when there are alterations in luggage weight or posture, the peak values and timing of the lumbar load can be accurately estimated. The correlation coefficient was 0.92.

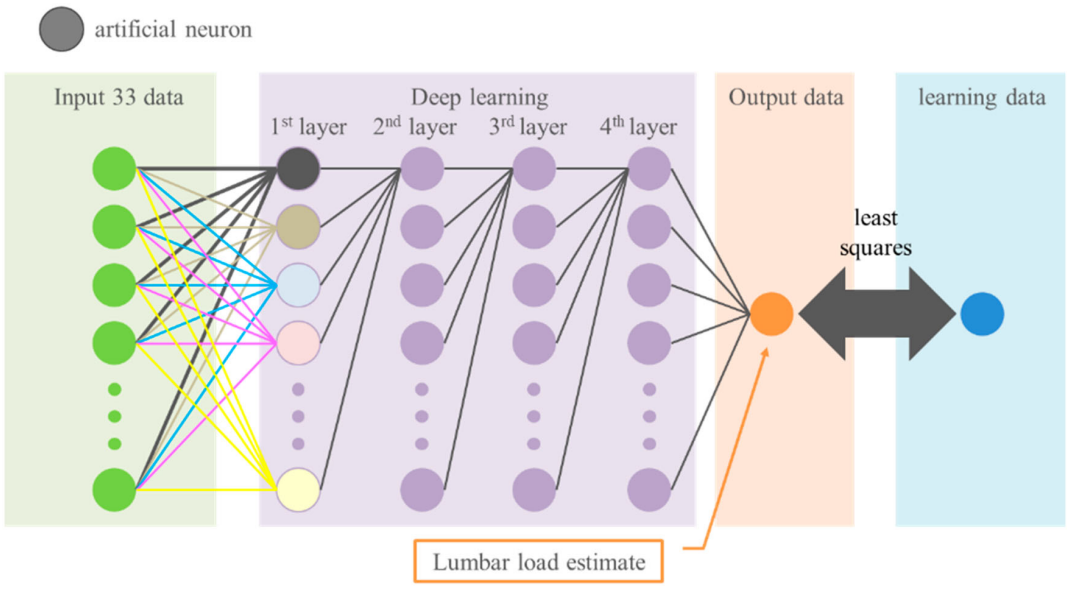

Figure 14. RNN.

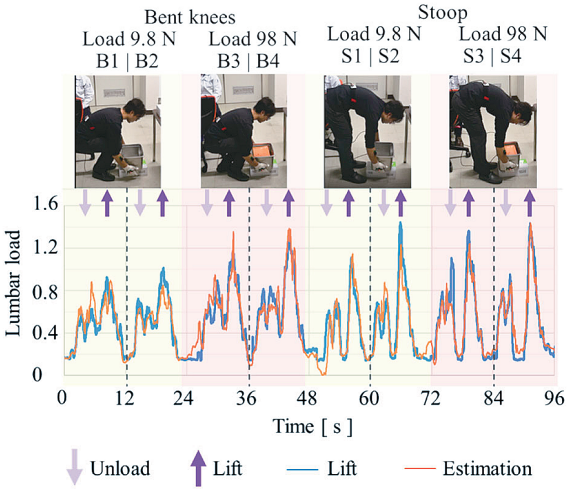

Figure 15. Estimated results utilizing verification data.

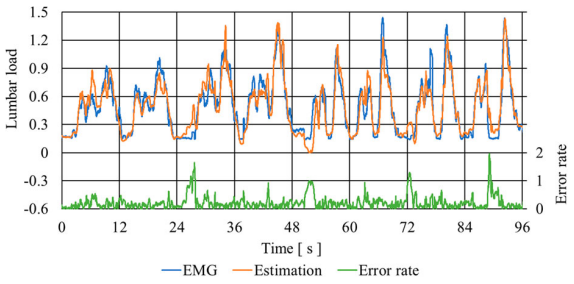

Figure 16. Error rate for each time period.

Focusing on the bent-knee posture (Figure 15; B1–B4), both the measured and estimated values demonstrated that the lumbar load increased with the weight of the luggage. The peak value when lifting a load increased significantly, and both the measured and estimated values exhibited the same tendency. For instance, the first (Figure 15; B3) and second (Figure 15; B4) lifts of a 98 N load involved the same motions; therefore, one would expect the peak values to be approximately equivalent. However, there was an experimental error of approximately 0.3 in the measured EMG values for both instances B3 and B4. Interestingly, while the peak values for the first (Figure 15; B3) and second (Figure 15; B4) lifts of the 98 N load exhibited similar experimental error of approximately 0.3 in the measured EMG values, the difference in estimates from the hand sensor device was approximately 0.05, which closely approximated the peak value.

Next, we examined the postural differences when the load weighed 9.8 N. Generally, the lumbar load showed a tendency to increase more during stooping (Figure 15; S1, S2) compared to the bent-knee posture (Figure 15; B1, B2), a trend also reflected in the estimated values. Similarly, the peak EMG values measured during the first and second lifting movements exhibited errors of approximately 0.3. In contrast, the error in the estimated values remained relatively stable at approximately 0.05.

Additionally, we calculated the error rate for each period (Figure 16). High error rates were observed between the unloading and lifting periods when the lumbar load was low. The mean and standard deviation of the error rate were approximately 0.21 and 0.23, respectively. Figure 17 shows a histogram of the error rates. The horizontal axis represents the error rates, whereas the vertical axis represents the frequencies (blue bars) and cumulative percentages (orange boxes). The cumulative error rates up to 0.2 was 63.2%, and up to 0.3 were 80.8%, respectively.

Furthermore, to assess the efficacy of the hand sensor device, we estimated the lumbar load using a limited number of sensors, as shown in Table 5. The simulation

Table 5. Explanatory variables used and error rate for max peak value.

		Acceleration		Quaternion		Bending		Stooping	
Type	Load	Hand	Lumbar	Hand	Lumbar	9.8 N	98 N	9.8 N	98 N
1	Use	Use	Use	Use	Use	−0.07	0.05	−0.03	0.01
2	–	Use	Use	Use	Use	0.04	−0.20	−0.08	−0.24
3	Use	–	–	Use	Use	−0.07	−0.03	0.03	0.11
4	Use	Use	Use	–	–	−0.03	−0.06	0.07	0.01
5	–	–	Use	–	Use	−0.26	−0.35	−0.15	−0.38
6	Use	Use	Use	–	–	−0.08	−0.09	−0.28	−0.20

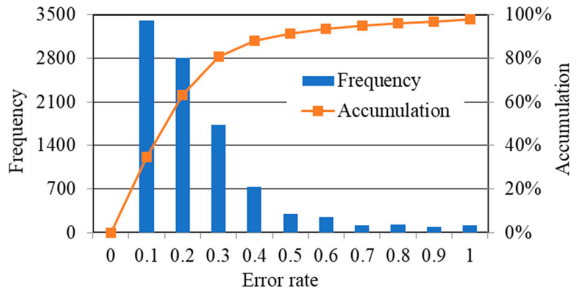

Figure 17. Histogram of error rate.

results are listed in the same table. Without the pressure sensor (Type 2), a significant error was observed in the peak value at 98 N. When the hand sensor device was not utilized (Type 5), substantial errors were observed in the peak values for all loads. Notably, a large error occurred during stooping when only the hand sensor device (Type 4) was utilized, and the nine-axis inertial sensor at the waist was not used. In contrast, the maximum error rate using all sensor values (Type 1) was 7%, underscoring the usefulness of the hand sensors.

4. Summary

We have developed a novel hand sensor device that mitigates sensor malfunction caused by flexion and corrects output values by considering palm hardness. Moreover, we attempted to estimate the lumbar load using deep learning based on the load information of the hand and posture information measured by the developed sensor. Through rigorous experimentation, we developed a highly accurate lumbar load estimation model. During a simple up-and-down motion, the estimated values closely matched EMG readings. The error rate of the estimation results was found to be approximately 7% at the peak value. Notably, the absence of even one sensor from the hand sensor device led to an increase in error rates.

Furthermore, during the experiment utilizing the myoelectric potential sensor, experimental errors arose owing to fluctuations caused by the fact that the EMG is a biological signal. However, the hand sensor device was designed to yield consistent and stable output, thereby confirming its usefulness.

These results confirm the usefulness of the hand sensor device.

Future endeavours will focus on expanding the subjects pool and introducing additional conditions, such as loads and motions. By conducting further experiments, we aim to broaden the scope of estimations achievable under real-world conditions.

A hand sensor device can enable real-time measurement of lumbar load, facilitating the control of assistive robots and fatigue management.

Acknowledgement

We would like to express our gratitude to Editage (www.editage.com) for their assistance with English language editing.

Disclosure statement

No potential conflict of interest was reported by the author(s).

Notes on contributors

Yusuke Yoshida (member) completed his Master's degree in Mechanical Engineering at Shizuoka University, Graduate School of Science and Engineering, in 2000. Following his tenure at a company, he later joined the Tottori Institute of Industrial Technology in 2009. His primary research interests include medical-engineering collaboration and system control. He is an active member of the SICE.

Takashi Kamezaki graduated from the Department of Industrial Arts at Kyoto Institute of Technology, Faculty of Industrial Arts, in 2011. He joined the Tottori Institute of Industrial Technology in the same year. His primary research interests include design and system control.

Dai Kinoshita (member) completed the second stage of the doctoral programme in engineering with an Interdisciplinary focus at Shimane University, Faculty of Science and Engineering, in 2021. That same year, he joined the faculty at the National Institute of Technology (KOSEN), Yonago College. His primary research interests are in the control of underactuated systems and control system design with state restrictions. Holding a Ph.D. degree, he is an active member of the SICE.

Daisuke Kushida (member) completed the second stage of the doctoral programme in production and control technology at Saga University (Graduate School of Science and Engineering) in 2002 and joined the faculty as a lecturer, assuming the position of a researcher in 2003. He subsequently assumed the position of research associate at Tottori University, where he has been an assistant professor in the Graduate School of Engineering since 2008, an associate professor at the Faculty of Engineering since 2018 and a professor at the Faculty of Engineering since 2022. His main research interests include modelling and quantification in the field of biomedical engineering. Holding a Ph.D. degree, he is an active member of SICE, IEEE, and various other professional societies.

References

[1] Status of Occupational Disease Occurrences compiled [Internet]. Japan: Ministry of Health, Labour and Welfare; Available from: https://www.mhlw.go.jp/stf/newpage_09976.html (in Japanese).

[2] Takeda K, Takagi N. Research on low back pain in care workers. Care Worker. 2016;20–21:90–102. (in Japanese).

[3] Balingit J, Iwase H, Kitaoka M. Working posture classification using a human body model in manual material handling. Jpn Ind Manage Assoc. 2004;55(2):77–88. (in Japanese).

[4] Seo A, Udo H, Yoshinaga F. Electromyogram measuring method for low back load evaluation of handling weight and forward bending posture. Jpn J Ind Health. 1993;35:19–24. (in Japanese).

[5] Kushida D, Kanazawa T, Kitamura A. Construction of lower limbs rehabilitation system based on bodily features and EMG. Inst Electr Eng Jpn. 2010;130(7):1132–1138. (in Japanese).

[6] Mita K. EMG measurement. J Jpn Soc Med Biol Eng BME. 1991;5(1):33–40. (in Japanese).

[7] Nakajima K, Anzai E, Iwakami Y, et al. Measuring gait pattern in elderly individuals by using a plantar pressure measurement device. Technol Health Care. 2014;22:805–815. doi:10.3233/THC-140856

[8] Seki Y, Shimojo M, Sato S, et al. Development of a grasping pressure distribution sensor with high flexibility. Trans Soc Instrum Control Eng. 1995;31(9):1528–1530. (in Japanese). doi:10.9746/sicetr1965.31.1528

[9] Sagisaka T, Ohmura Y, Nagakubo A, et al. High-density conformable tactile sensing glove. J Rob Soc Jpn. 2012;30(7):711–717. (in Japanese).

[10] Yoshida Y, Kamezaki T, Kinoshita D, et al. Development of hand sensor device for lumbar load estimation. Proceedings of the 62nd Annual Conference of the SICE. 2023; p. 66–71.

[11] Japanese Society for Surgery of the Hand. Hand surgery glossary. Japan: NAP Limited; 2012; (in Japanese).

[12] Yoshida Y. Prediction of grasping force of workers by removable simple hand sensor. Proceedings of the 26th Annual Conference of the SICE Chugoku Chapter. 2017; 26:85–86. (in Japanese).